Recent development of neutron and energetic-particle diagnostics for LHD deuterium discharges

M. Isobe,[a,b] K. Ogawa,[a,b] S. Sangaroon,[c] S. Kamio,[a] Y. Fujiwara, [d] and M. Osakabe[a,b]

[a] *National Institute for Fusion Science, National Institutes of Natural Sciences*
322-6 Oroshi-cho, Toki-shi, Gifu, 509-5292, Japan
[b] *The Graduate University for Advanced Studies, SOKENDAI*
322-6 Oroshi-cho, Toki-shi, Gifu, 509-5292, Japan
[c] *Mahasarakham University*
20 41 Kham Riang, Kantharawichai District, Maha Sarakham 44150, Thailand
[d] *NTT Space Environment and Energy Laboratories*
3-9-11 Midori-cho, Musashino-shi, Tokyo 180-8585, Japan

E-mail: isobe.mitsutaka@nifs.ac.jp

ABSTRACT: An integrated set of neutron diagnostics developed for the deuterium operation of the Large Helical Device (LHD) has been revealing behavior of energetic ions in three-dimensional plasmas, together with energetic-particle diagnostics. In order to obtain deeper understanding of physics related to energetic ions in the LHD, development of plasma diagnostics that can provide energy distribution of energetic ions is now being accelerated. Recent advances in development of the D-D neutron energy spectrometer, a neutral particle analyzer based on a single-crystal chemical vapor deposition diamond, and a tangential fast-ion Dα diagnostic for deuterium discharges of the LHD are described.

KEYWORDS: Large Helical Device; Nuclear fusion; Deuterium plasma; Neutron; Energetic particle

Contents

1. Introduction

Energetic particles have been primary measurement and physics targets in magnetic confinement fusion since the D-T born 3.5 MeV alpha particle plays an essential role in sustaining the self-ignition condition in a future DEMO and/or commercial nuclear fusion reactor. In particular, the confinement property of energetic particles has been of great concern in stellarator/heliotron devices because of a lack of symmetry of the system leading to ripple transport. For this reason, a variety of energetic-particle diagnostics were developed and operated in the early and middle stages of the LHD project [1]. An integrated set of charge-exchange neutral-particle analyzers (NPAs), i.e., solid-state NPAs such as natural diamond detectors (NDDs) [2,3] and silicon detectors [4,5], conventional NPAs such as the E//B type [6,7], the time-of-flight type [8], and the compact NPA using a strong permanent magnet [9] were operated for understanding energetic-ions' behavior in the LHD [10] together with the scintillator-based escaping energetic-ion diagnostic [11]. These detectors had been working as key energetic-particle diagnostics in the hydrogen plasma regime of the LHD. Subsequently, the LHD project entered the final stage in March 2017 to realize high-performance plasmas with deuterium gas, to investigate the isotope effect, and to demonstrate the confinement capability of energetic ions in a non-axisymmetric system [12,13]. In the deuterium plasma regime, D-D born neutrons have become a new measurement target for energetic-ion studies in the LHD, in addition to assessment of fusion gain. Neutral-beam (NB)-driven D-D neutrons are dominant in the total neutron emission rate in the LHD, like any other fusion experiment devices where NB heating is performed [13]. Therefore, an integrated set of neutron diagnostics, consisting of a neutron flux monitor [14] and a neutron activation system [15] for the neutron emission rate and/or yield measurement, a vertical neutron camera (VNC) [16] for profile measurement of NB-injected energetic ions, hereafter beam ions, a scintillating-fiber detector [17] for secondary D-T neutron emission rate measurement, and a neutron fluctuation diagnostic [18] had been developed prior to the start of the deuterium operation. Those diagnostics have been successfully operated in enhancement of energetic-ion physics studies in LHD plasmas [19-21]. In order to obtain deeper understanding of the slowing down process of beam ions, and the interaction between beam ions and beam-ion-driven magnetohydrodynamics (MHD) instabilities, information on beam ions' energy distribution is essential. However, so far it has been lacking diagnostics to measure the energy distribution of

beam ions confined in a plasma. For this purpose, lately we have begun to develop D-D neutron energy spectrometers. Also, NPAs and a fast-ion Dα diagnostic (so-called FIDA) have been largely enhanced in the LHD. In this paper, recent advances of neutron and energetic-ion diagnostics development in the LHD are described.

2. Motivation for beam ions' energy distribution measurement

Interplay between energetic ion and energetic-ion-driven MHD instabilities is intensively investigated in existing toroidal fusion devices. This is because those MHD instabilities can potentially expel energetic alphas, leading to a loss of the self-ignition condition and significant damage to plasma facing components in a future fusion burning plasma. Because of this background, in the LHD, studies on energetic-ion-driven MHD instabilities such as the toroidicity-induced Alfvén eigenmode (TAE) [22,23], the helicity-induced Alfvén eigenmode (HAE) [24], the energetic-particle continuum mode (EPM) [25], the resistive interchange mode destabilized by helically trapped energetic ions (EIC) [26,27], and the energetic-particle-driven geodesic acoustic mode (EGAM) [28,29] have been conducted. As an example, a discharge associated with energetic-ion-driven MHD instabilities resulting in beam ion loss is shown in Fig. 1. In the hydrogen operation phase of the LHD, energetic-ion-driven MHD instabilities were preferably destabilized when intensive tangential negative-ion-source based neutral beams (N-NBs) were injected in a low toroidal magnetic field strength (B_t) condition, resulting in high beam ion beta. It was found that this characteristic in a deuterium plasma was the same as in a hydrogen plasma. In this particular shot, recurrent bursts appeared when two deuterium N-NBs were co- and counter-injected into the deuterium plasma of the LHD. Each burst was accompanied by a frequency downshift. Associated with each mode burst, the total neutron emission rate (S_n)

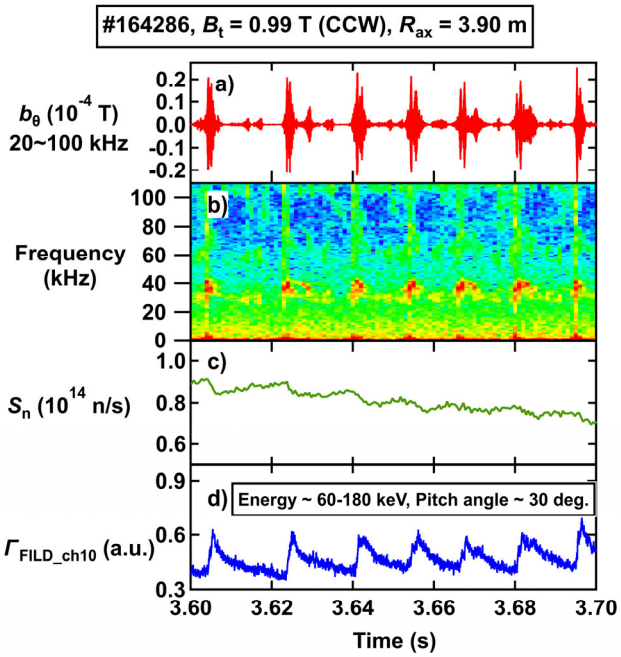

Fig. 1. Waveforms of plasma discharge while energetic-ion-driven MHD modes destabilized by balance injection of N-NBs. a) Amplitude of magnetic fluctuation, b) Magnetic spectrogram, c) Total neutron emission rate, d) escaping beam ion flux.

measured with a neutron fluctuation detector decreased, whereas escaping beam ion flux measured inside the vacuum chamber increased as can be seen in Fig. 1. This observation tells us that the instabilities were destabilized by tangentially injected beam ions and expelled beam ions responsible for the mode excitation.

Generally speaking, excitation of energetic-ion-driven MHD instabilities is tightly connected to the kinetics of beam ions such as the pressure profile and energy distribution function. After the start of the deuterium operation, the VNC in the LHD provided valuable information to increase understanding of the mode excitation condition, i.e., spatial distribution of beam ions which was unavailable in the hydrogen phase, through the measurement of the neutron emission profile. A significant change of the beam ions' profile before/after the excitation of energetic-ion-driven MHD instabilities was indicated [30,31]. This observation tells us that the mode excitation condition is associated with the pressure profile of beam ions. In the JET, measurements of energetic ions and their interactions with MHD activity using neutron spectroscopy were performed and the energy range of energetic ions responsible for the mode excitation was revealed experimentally [32]. As this example has shown, information on the energy distribution of energetic ions confined in LHD plasmas is required to step into further understanding of the excitation mechanism of energetic-ion-driven MHD instabilities. Based on this motivation, we have initiated development of the D-D neutron spectrometer, and enhancement of NPAs and the fast-ion Dα diagnostic.

3. Recent diagnostics development for measurement of beam ions' energy distribution

3.1. Compact D-D neutron energy spectrometer

The tangential compact D-D neutron energy spectrometer (CNES), based on the recently developed ^{7}Li-enriched Cs_2LiYCl_6:Ce (CLYC7) fast-neutron scintillator, is installed in the LHD for the purpose of measuring the energy distribution of passing transit beam ions [33]. The advantage of the CLYC7 scintillator over the conventional liquid scintillator is that the CLYC7 can directly provide neutron energy using a ^{35}Cl reaction, such as ^{35}Cl(n,p)^{35}S. A CLYC7 crystal of 1-inch diameter and 1-inch height, directly coupled with a 1-inch photomultiplier tube (PMT), is utilized as the CLYC7 detector. Figure 2 shows the top view of the LHD with the CNES. The tangency radius of the sightline of the CLYC7 detector is set to be 3.65 m. The beam ions injected by N-NB#1, having a tangential radius of 3.75 m, move toward the CLYC7 detector. The CLYC7 detector is immersed in the shielding box, consisting of 10 mm thick iron, for avoiding the unfavorable magnetic field effect on the PMT, 50 mm thick lead for gamma-ray shielding, and 10% borated polyethylene for scattered neutron shielding. The anode signal of the PMT is directly fed into the data acquisition system, equipped with a 250 MHz sampling analog-to-digital convertor, and the field programmable gate array, having online pulse shape discrimination (PSD) ability (DT5720B, CAEN). The discrimination between neutron-induced signals and gamma-ray-induced ones is performed by using the difference in the decay time of the pulse signal. We measured the neutron energy spectrum in a tangential N-NB-heated deuterium plasma with B_t of 1.375 T in a counterclockwise direction from the top view and magnetic axis position in a vacuum (R_{ax})=3.75 m. Short pulse deuterium N-NB#1 was injected into relatively low-density electron cyclotron resonance heated deuterium plasma (Fig. 3). Here, the bulk plasma parameters, e.g., the central electron temperature (T_{e0}) and the line-averaged electron density (n_{e_avg}), were almost unchanged at the time of interest. S_n increases with the N-NB#1 injection and decays after N-

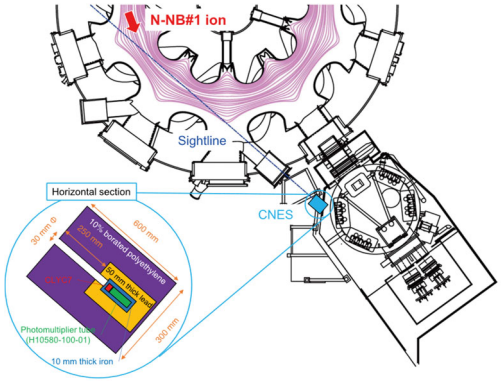

Fig. 2 Top view of LHD together with CNES. Beam ions injected by N-NB#1 move toward CNES.

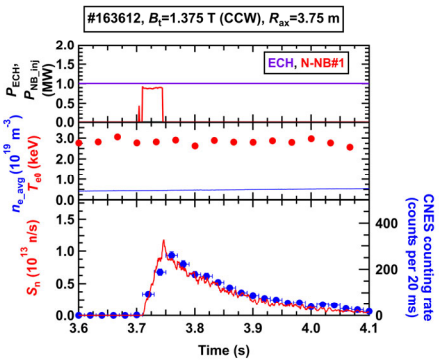

Fig. 3 Waveform of deuterium N-NB heated deuterium discharge, where D-D neutron spectrum was measured.

NB#1 stops. The decay of S_n is observed due to the slowing down and transport of beam ions. The time trend of the pulse counting rate of the CNES almost matches with the time trend of S_n. Here, the expected pulse pileup rate is negligibly small < 2% because the typical pulse width of the CLYC7 detector is ~1 μs. A two-dimensional plot of PSD, which reflects the decay time of the pulse signal, as a function of the charge integral to the pulse signal (Q_{total}) is shown in Fig. 4 a). The neutron signal, which corresponds to a high PSD ~0.57, is separated from the gamma-ray signal corresponding to a lower PSD ~0.5. Figure 4 b) shows the neutron energy spectra measured by the CLYC7 detector in the experiment and calculated based on the orbit following model DELTA5D code [34]. The error bar in D-D neutron counts shows the statistical error of counts. The Gauss fitting shows that the peak energy of D-D neutrons is largely shifted to 2.87 MeV. Note that the D-D neutron energy created by two static deuterons is 2.45 MeV. In the neutron flux calculation, beam ion distribution was calculated by the guiding center orbit following model in the Boozer coordinates. The number of beam ions and orbit following time were set to be 10^5 and one second, respectively. And then the energy of D-D neutrons arriving at the CLYC7 detector was calculated by considering the CLYC7 sight lines and by including the double differential cross section of the D-D reaction [35, 36]. It was found that the peak energy of the neutron flux in the calculation ~2.92 MeV was close to the peak energy obtained in the experiment ~2.87 MeV. The response of the CLYC7 detector, e.g., sensitivity and energy resolution, will be included for

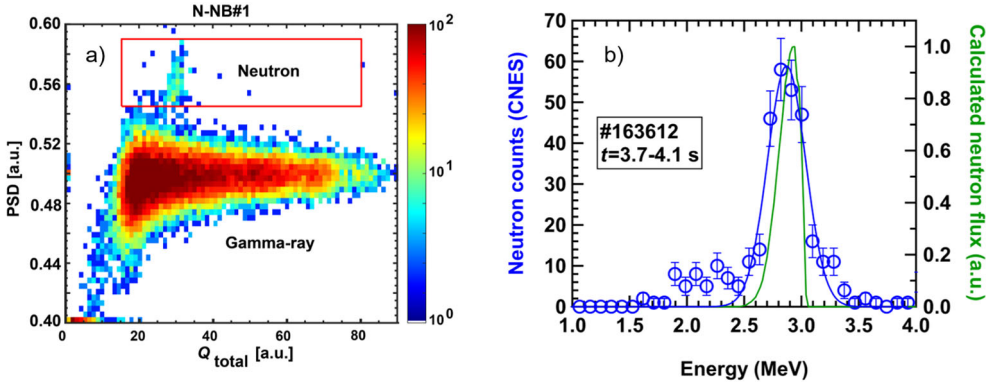

Fig. 4 a) Two-dimensional pulse shape discrimination plot obtained by CLYC7 detector. b) Neutron energy spectra measured in experiment and calculated based on orbit following model.

a detailed comparison of the neutron spectrum in order to understand the beam ion energy distribution inside the plasma.

3.2. Neutral particle analyzer based on single-crystal chemical vapor deposition diamond

The LHD is equipped with various NPAs from the operation phase with hydrogen gas [1]. As the start of the deuterium operation, we enhanced performance of an E//B-type NPA in terms of high time resolution [37]. Also we newly introduced single-crystal chemical-vapor-deposition (CVD) diamonds as an NPA [38]. It is known that a diamond has favorable characteristics in terms of radiation hardness and operation capability in a high-temperature environment. Therefore, it can be said that a diamond detector is suitable for a deuterium plasma diagnostic. We had used NDDs as a compact NPA in the hydrogen phase [2]. Since there has been an issue on procurement of NDDs, we have switched to a single-crystal CVD diamond detector which is now commercially available. Four single-crystal CVD diamond detectors (B12 Diamond Knopf Detector, CIVIDEC Instrumentation) are being employed in the LHD at this moment, as seen in Fig. 5. The sensitive area of the diamond detector is 4 mm × 4 mm. These detectors view the plasma perpendicularly from the bottom side of the machine, where the elliptical poloidal cross section is slightly tilted in order to observe helically trapped energetic ions originating in perpendicular NB injection or produced by ion cyclotron range of frequency (ICRF) wave heating. Helically trapped energetic ions, confined magnetically in the valley of the two helical winding coils, are of great concern with respect to their confinement property because of a lack of symmetry of the system. A pseudo pulse due to neutron irradiation had been our great anxiety. According to a preliminary survey at the accelerator-type fast neutron source facility of Tohoku University and the experiences at the LHD, we have concluded that contamination due to a neutron-induced pseudo signal is not significant in the LHD environment [39]. Energy distributions of the charge-exchanged energetic-ion tail are measured by use of single-crystal CVD diamond detectors in ICRF discharges (SN169850-169859). The experiments were performed with an ICRF frequency of 38.47 MHz in

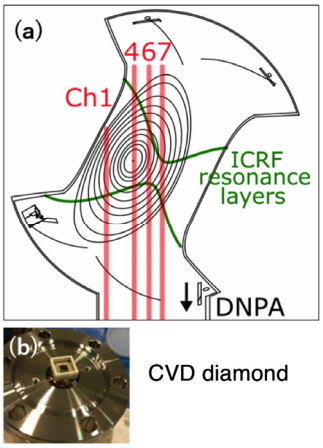

Fig. 5 a) Lines of sight of single-crystal CVD diamond detectors together with ICRF resonance layers. b) External appearance of CVD diamond detector, placed 7.77 m below the equatorial plane of LHD.

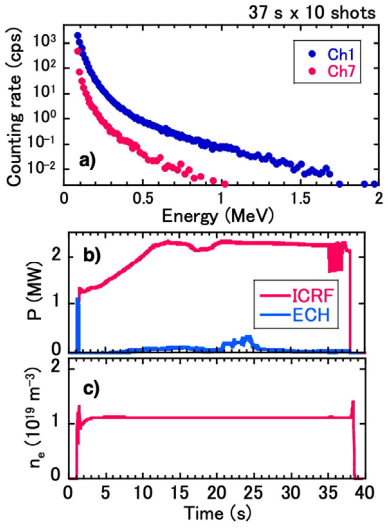

Fig. 6 a) Energy distributions of helically trapped energetic-ion tails produced by ICRF wave measured by single-crystal CVD diamond detectors Ch. 1 and Ch. 7. b) Time evolutions of injection powers of ICRF wave and electron cyclotron heating (ECH), (c) Line-averaged electron density.

hydrogen minority and deuterium majority plasmas in B_t=2.75 T in a counterclockwise direction from the top view and R_{ax}=3.60 m. The result shows that fundamental proton minority heating by an ICRF wave with ~2 MW injection power effectively produces a suprathermal proton tail over 1.5 MeV, as seen in Fig. 6a). The energy of tail ions measured in outboard sightline Ch. 7 is lower than in inboard sightline Ch.1. Analysis to understand the mechanism of asymmetry of the energetic-ion tail formation is in progress.

3.3. Tangential fast-ion Dα diagnostic

In the LHD, TAEs are often destabilized when N-NB is tangentially co-injected. Therefore, the radial profile and velocity distribution of passing beam ions are of inherent interest. Based on this background, efforts on development of tangential FIDA are now being made. In the FIDA diagnostic, the Doppler-shifted Dα lights from fast neutrals are utilized as signals of fast ions, where these fast neutrals are produced by the charge exchange process between fast ions existing in plasmas and actively introduced fast neutrals by NB injection. The advantage of the FIDA diagnostic is the local measurement at crossing points between its lines of sight and the incident line of NB injection. The latest FIDA numerical calculation model FIDASIM, which has been improved to be suitable for a three-dimensional magnetic field configuration, has been applied in the LHD to understand the phase space distribution of beam ions in stellarator/helical devices [40, 41]. Here, we briefly report the comparison of the spectra obtained by tangential FIDA diagnostics in an MHD-quiescent deuterium plasma experiment and calculated with FIDASIM, using beam ion distribution by drift kinetic equation solver GNET code [42]. The experiment was conducted in R_{ax} of 3.6 m, and B_t of 2.75 T in a counterclockwise direction from the top view. Energetic deuterium was tangentially co-injected by N-NB, resulting in passing beam ions in a plasma. The FIDA measurement was performed by the modulation injection of positive-ion-source-based NB (P-NB) to subtract the background signal. Here, the injection energies of N-NB and P-NB were ~147 keV and ~57 keV, respectively. Figure 7 shows the net signal obtained by FIDA diagnostics (black line) and theoretical radiance of various spectral components calculated by the FIDASIM at R=3.597 m in the discharge SN146696. Note that the intensity of the FIDA signal obtained in the experiment was arbitrary units, using a calibration factor (f_{calib}) to attempt a relative comparison between the experimental and numerical results. The red solid line stands for the direct charge exchange (DCX) component signal which comes from the charge exchange reaction between beam neutrals and thermal ions. The yellow solid line represents the beam emission spectroscopy (BES) component signal including the full, half, and one third energy component of the beam. The green solid line is for the HALO signal which comes from newly created thermal neutrals which travel ballistically and charge exchange with other thermal ions, creating more neutrals after neutralization. The blue solid line is the FIDA component. The violet solid line is the total radiance of spectra by the FIDASIM. As a result of the comparison of the FIDA diagnostic with FIDASIM results, they are in good agreement. This result indicates that the FIDA diagnostic is a strong tool for understanding beam-ion distribution, not only in the two-dimensional magnetic field device, but also in the three-dimensional one. In future work, we will understand beam-ions' behavior with MHD instabilities using the FIDA diagnostic and the FIDASIM in the LHD.

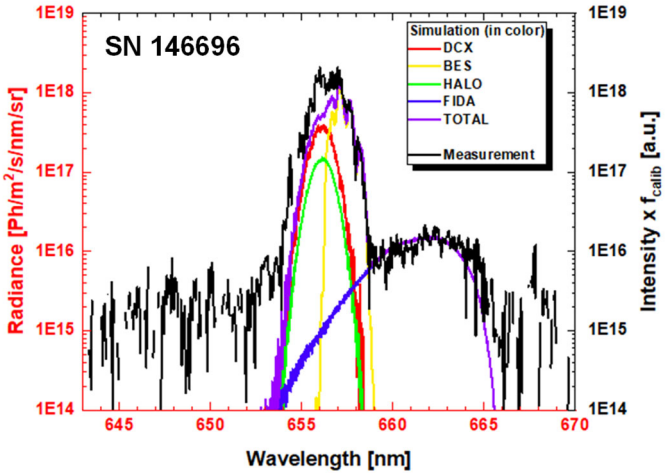

Fig. 7 Measured spectra by FIDA diagnostic and various Dα components calculated by FIDASIM in case of N-NB injection at R=3.597 m in discharge SN146696.

4. Summary

Understanding the physics of energetic ion confinement, e.g., ripple-induced radial transport and/or loss and interaction between energetic ions and energetic-ion-driven MHD instabilities is crucial for obtaining a positive perspective towards realization of helical-type nuclear fusion reactors. We have been conducting energetic-ion physics experiments in the LHD by means of an integrated set of neutron and energetic-particle diagnostics. Since a weakness in the LHD has been plasma diagnostics to provide energy distribution of beam ions, development of D-D neutron energy spectrometers, NPAs based on a single-crystal CVD diamond, and tangential FIDA are being accelerated. Those diagnostics have been set up steadily and are meeting our expectations.

Acknowledgments

This work was supported by the NINS program of Promoting Research by Networking among Institutions (Grant No. 01411702), by Japan/US and Japan/China Cooperations in Fusion Research and Development. We are pleased to acknowledge the assistance of the LHD Experiment Group.

Data availability statement

The LHD data can be accessed from the LHD data repository at https://www-lhd.nifs.ac.jp/pub/Repository_en.html

References

[1] M. ISOBE et al., *FAST-PARTICLE DIAGNOSTICS ON LHD*, *Fusion Sci. Technol.* **58** (2010) 426.

[2] M. Isobe et al., *Charge exchange neutral particle analysis with natural diamond detectors on LHD heliotron*, *Rev. Sci. Instrum.* **72** (2001) 611.

[3] T. Saida et al., *Study of ripple-trapped proton behaviour in LHD by two line-of-sight measurements of fast neutrals*, *Nucl. Fusion* **44** (2004) 488.

[4] M. Osakabe et al., *Development and energy calibration of Si-FNA for LHD fast ion measurement, Rev. Sci. Instrum*. **72** (2001) 788.

[5] J.F. Lyon et al., *Spatially resolved measurements of energetic neutral particle distributions in the Large Helical Device*, *Rev. Sci. Instrum*. **74** (2003) 1873.

[6] S.S. Medley et al., *Construction and operation of parallel electric and magnetic field spectrometers for mass/energy resolved multi-ion charge exchange diagnostics on the Tokamak Fusion Test Reactor, Rev. Sci. Instrum*. **69** (1998) 2651.

[7] M. Osakabe et al., *Evaluation of energetic particle confinement using CXNPA with NB-blip experiments on Large Helical Device, Rev. Sci. Instrum.* **75** (2004) 3601.

[8] T. Ozaki et al., *High-energy neutral particle measurement system in the large helical device, Rev. Sci. Instrum*. **71** (2000) 2698.

[9] P.R. GONCHAROV et al., *ACTIVE NEUTRAL PARTICLE DIAGNOSTICS ON LHD BY LOCALLY ENHANCED CHARGE EXCHANGE ON AN IMPURITY PELLET ABLATION CLOUD, Fusion Sci. Technol*. **50** (2006) 222.

[10] M. OSAKABE et al., *FAST-ION CONFINEMENT STUDIES ON LHD, Fusion Sci. Technol.* **58** (2010) 131.

[11] T. Saida et al., *ESCAPING ENERGETIC ION MEASUREMENT ON LARGE SCALE MAGNETIC FUSION DEVICES, Advanced Diagnostics for Magnetic and Inertial Fusion*, Edited by Stott et al. Kluwer Academic/Plenum Publishers, New York, 2002, p133.

[12] Y. Takeiri, *Prospect Toward Steady-State Helical Fusion Reactor Based on Progress of LHD Project Entering the Deuterium Experiment Phase, IEEE Trans. Plasma Sci*. **46** (2018) 1141.

[13] M. Osakabe et al., *Preparation and Commissioning for the LHD Deuterium Experiment, IEEE Trans. Plasma Sci*. **46** (2018) 2324.

[14] M. Isobe et al., *Wide dynamic range neutron flux monitor having fast time response for the Large Helical Device, Rev. Sci. Instrum*. **85** (2014) 11E114.

[15] N. Pu et al., *In situ calibration of neutron activation system on the large helical device, Rev. Sci. Instrum*. **88** (2017) 113302.

[16] K. Ogawa et al., *Progress in development of the neutron profile monitor for the large helical device, Rev. Sci. Instrum.* **85** (2014) 11E110.

[17] K. Ogawa et al., *Time-resolved triton burnup measurement using the scintillating fiber detector in the Large Helical Device, Nucl. Fusion* **58** (2018) 034002.

[18] Kunihiro OGAWA et al., *Neutron Flux Measurement Using a Fast-Neutron Scintillation Detector with High Temporal Resolution on the Large Helical Device, Plasma Fus. Res.* **13** (2018) 3402068.

[19] M. Isobe et al., *Fusion neutron production with deuterium neutral beam injection and enhancement of energetic-particle physics study in the large helical device, Nucl. Fusion* **58** (2018) 082004.

[20] Mitsutaka Isobe et al., *Neutron Diagnostics in the Large Helical Device, IEEE Trans. Plasma Sci*. **46** (2018) 2050.

[21] K. Ogawa et al., *Energetic ion confinement studies using comprehensive neutron diagnostics in the Large Helical Device, Nucl. Fusion* **59** (2019) 076017.

[22] K. Ogawa et al., *Magnetic configuration effects on TAE-induced losses and a comparison with the orbit-following model in the Large Helical Device*, *Nucl. Fusion* **52** (2012) 094013.

[23] K. Ogawa et al., *A study on the TAE-induced fast-ion loss process in LHD, Nucl. Fusion* **53** (2013) 053012.

[24] S. Yamamoto et al., *Observation of Helicity-Induced Alfvén Eigenmodes in Large-Helical-Device Plasmas Heated by Neutral-Beam Injection, Phys. Rev. Lett*. **91** (2003) 245001

[25] M. Isobe et al., *Effect of Energetic-Ion-Driven MHD Instabilities on Energetic-Ion-Transport in Compact Helical System and Large Helical Device, Contrib. Plasma Phys*. **50** (2010) 540.

[26] X.D. Du et al., *Resistive Interchange Modes Destabilized by Helically Trapped Energetic Ions in a Helical Plasma, Phys. Rev. Lett*. **114** (2015) 155003.

[27] X.D. Du et al., *Resistive interchange mode destabilized by helically trapped energetic ions and its effects on energetic ions and bulk plasma in a helical plasma, Nucl. Fusion* **56** (2016) 016002.

[28] T. Ido et al., *Potential fluctuation associated with the energetic-particle-induced geodesic acoustic mode in the Large Helical Device, Nucl. Fusion* **51** (2011) 073046.

[29] T. Ido et al., *Identification of the energetic-particle driven GAM in the LHD, Nucl. Fusion* **55** (2015) 083024.

[30] K. Ogawa et al., *Observation of enhanced radial transport of energetic ion due to energetic particle mode destabilized by helically-trapped energetic ion in the Large Helical Device, Nucl. Fusion* **58** (2018) 044001.

[31] K. Ogawa et al., *Effect of the helically-trapped energetic-ion driven resistive interchange modes on energetic ion confinement in the Large Helical Device, Plasma Phys. Control. Fusion* **60** (2018) 044005.

[32] C. Hellesen et al., *Measurements of fast ions and their interactions with MHD activity using neutron emission spectroscopy, Nucl. Fusion* **50** (2010) 084006.

[33] S. Sangaroon et al., *Neutron Energy Spectra Measurement using CLYC7-based Compact Neutron Emission Spectrometer in the Large Helical Device*, *JINST* **16** (2021) C12025.

[34] D. A. Spong et al., *Three-dimensional effects on energetic particle confinement and stability, Phys. Plasmas* **18** (2011) 056109.

[35] S. Sugiyama et al., *Observation of neutron emission anisotropy by neutron activation measurement in beam-injected LHD deuterium plasmas, Nucl. Fusion* **60** (2020) 076017.

[36] P. R. Goncharov, *Differential and total cross sections and astrophysical S-factors for $^{2}H(d,n)^{3}He$ and $^{2}H(d,p)^{3}H$ reactions in a wide energy range, At. Data Nucl. Data Tables* **120** (2018) 121.

[37] Y. Fujiwara et al., *Enhancement of an E parallel B type neutral particle analyzer with high time resolution in the Large Helical Device*, *JINST* **15** (2020) C02021.

[38] S. Kamio et al., *Development of NPA array using single crystal CVD diamond detectors*, *JINST* **14** (2019) C08002.

[39] S. Kamio et al., *Neutron-induced signal on the single crystal chemical vapor deposition diamond-based neutral particle analyzer, Rev. Sci. Instrum*. **91** (2020) 113304.

[40] Y. Fujiwara et al., *Evaluation of an Energetic Particle Profile Using a Tangential-FIDA Diagnostic in the Large Helical Device, Plasma Fus. Res.* **14** (2019) 3402129.

[41] Y. Fujiwara et al., *Fast-ion D alpha diagnostic with 3D-supporting FIDASIM in the Large Helical Device, Nucl. Fusion* **60** (2020) 112014.

[42] H. Yamaguchi and S. Murakami, *Simulation study of NBI heating in the time-evolving and multi-ion-species plasmas of LHD, Nucl. Fusion* **56** (2016) 026003.